Effect of rare-earth (R = Pr, Gd, Ho, Er) doping on the Magnetostructural phase transitions and magnetocaloric properties in $Ni_{43-x}R_xMn_{46}Sn_{11}$ shape memory alloys

Anil Aryal [1, *], Sudip Pandey [1], Igor Dubenko [1], Dipanjan Mazumdar [1], Shane Stadler [2], and Naushad Ali [1]

[1]Department of Physics, Southern Illinois University, Carbondale, IL 62901, USA

[2]Department of Physics & Astronomy, Louisiana State University, Baton Rouge, LA 70803, USA

ABSTRACT:

A series of rare-earth doped $Ni_{43-x}R_xMn_{46}Sn_{11}$ (x = 0, 1 and R = Pr, Gd, Ho) alloys were fabricated by arc-melting method and their structural, magnetic and magnetocaloric properties were studied through room temperature X-ray diffraction (XRD), differential scanning calorimetry (DSC) and magnetization measurements. Analysis of XRD data reveals that the alloys crystallize in the cubic $L2_1$ austenite (AP) as major phase with small trace of martensitic phase (MP). The martensitic transition temperature (T_M) shifts towards higher temperature by the corresponding substitution of Pr, Gd, Ho, and Er. A drastic shift in T_M by ~ 60 K relative to the parent compound (T_M = 195 K) was found for $Ni_{42}PrMn_{46}Sn_{11}$alloy. Large values of magnetic entropy changes (ΔS_M) of 32 $Jkg^{-1}K^{-1}$(Pr), 28 $Jkg^{-1}K^{-1}$ (Gd), and 25 $Jkg^{-1}K^{-1}$ (Ho) were obtained at T_M for ΔH = 5 T. Maximum value of refrigeration capacity (RC) of ~ 250 J kg^{-1} was obtained in the vicinity of T_M for ΔH = 5 T for Ho doped compound. Large exchange bias effect with H_{EB} ~ 1.1 kOe at 10 K was observed for Pr doped compound in its MP. Moderate magnetoresistance (~ -20 %) was observed for $Ni_{42}GdMn_{46}Sn_{11}$ alloy near T_M for the magnetic field change of 5 T.

INTRODUCTION:

The magnetocaloric effect (MCE) is an adiabatic temperature change (ΔT_A) or isothermal magnetic entropy change (ΔS_M) in a magnetic material, induced by an applied magnetic field. Magnetocaloric effect (MCE) has been a subject of intense investigation due to its potential application in magnetic refrigeration, a solid-state cooling technology that is environmentally friendly and efficient compared to traditional gas compressed refrigerators [1, 2]. However successful development of this technology requires discovery of new materials that is less expensive and show large MCE near room temperature. Extensive research are being conducted on some material systems that undergo a first-order magnetostructural transitions (MSTs) and show giant MCEs such as $Gd_5Si_2Ge_2$, MnFe(P,As), $LaFe_{13-x}Si_x$, and $MnAs_{1-x}Sb_x$ and NiMnX (X = Ga, Sn, Sb, In) Heusler alloys [3-11].

Recently off-stoichiometric Ni-Mn-X (X = In, Sn, Sb) based Heusler alloys have received considerable attention because they undergo a first-order martensitic transitions (MT) from high symmetry (cubic $L2_1$-type) austenite phase (AP) to a low symmetry (10 M, 14 M, or $L1_0$) martensitic phase (MP) [7, 8, 11]. These alloys show remarkable magnetoresponsiveproperties such as magnetic shape memory effect, exchange bias, large magnetoresistance, and large magnetocaloric effects [7, 9, 12-18] associated with the MT. It has been reported that MT temperature in these alloys can be tuned by changing the chemical composition of alloy or doping of extra elements. The valance electron concentration per atom (e/a) and the distance between the Mn-Mn atoms are considered as the major factor affecting the structural and magnetic properties of the Ni-Mn-X-based Heusler alloys [8, 11, 19]. These factors can modify the electronic band structure and affect the phase transitions and the associated phenomena [11]. However, the exact mechanisms responsible for the unique behaviors shown by these alloys are

not clear. Thus, studies of the influence of doping on the physical properties can provide new information important for understanding the behavior, and their applicability in new technological areas.

Up to date, the reports on the effect of rare-earth element doping on the phase transitions and magnetic entropy changes in Ni-Mn-X based Heusler alloys are limited. In this work, we present the results of doping rare-earth elements (R = Pr, Gd, Ho, and Er) in the $Ni_{43-x}R_xMn_{46}Sn_{11}$(x = 0, 1) Heusler system.

EXPERIMENTAL TECHNIQUES

Approximately 4 gm of polycrystalline samples with nominal compositions were fabricated by arc-melting high purity starting elements (99.99%) in an ultra-high purity argon atmosphere. The details of sample synthesis procedure and handling of rare-earth (RE) metal are published elsewhere [20]. The ingots were then wrapped in tantalum foil and annealed in high vacuum (~10^{-4}Torr) for 48 hrs at 850 ^{o}C and slowly cooled down to room temperature. The phase purity and crystal structure were were obtained by a high resolution Rigaku Smart Lab X-ray diffractometer using CuKα radiation at room temperature. The magnetization and resistivity (four-probe method) were measured using a SQUID magnetometer (Quantum Design) in the temperature interval 5 - 380 K, and in applied magnetic fields up to 5T. Magnetic measurements were taken following the protocols as: The samples were first cooled to 10 K from 400 K at zero field. The zero-field-cooling (ZFC) measurements were taken while heating the samples to 400 K in an applied magnetic field, and then followed by field-cooled-cooling (FCC) measurement to 10 K and field-cooled-heating (FCH) measurement from 10 K to 400 K. The phase transition temperatures were determined from the minimum of the dM/dT vs. T curves in M(T) during the

heating cycle. Differential scanning calorimetry (DSC) measurements were carried out using a DSC 8000 instrument (Perkin-Elmer) with a ramp rate of 20 K / min during heating and cooling, and in the temperature range 123 - 423 K. The latent heat (L) was estimated from the endothermic peaks of the heat flow curves using the equation, $L = \int_{T_s}^{T_f} \frac{dQ}{dT} dT$, where $\frac{dQ}{dT}$ is the change in heat flow with respect to temperature, and T_s and T_f are initial and final temperatures of the structural phase transition on heating, respectively. The total entropy changes (ΔS_T) was calculated using $\Delta S_T = L / T_M$, where L is the latent heat in J kg^{-1} and T_M is the martensitic transition temperature in K corresponding to the peak position in the DSC heat flow curves.

RESULTS AND DISCUSSION:

Fig. 1 (a) shows the room temperature X-ray diffraction patterns of the parent $Ni_{43}Mn_{46}Sn_{11}$ and the rare-earth doped $Ni_{42}RMn_{46}Sn_{11}$ (R = Pr, Gd, Ho, Er) alloys. The diffraction peaks observed for all samples at room temperature can be identified in cubic $L2_1$ austenitic as main phase. However, a small trace of martensitic phase (MP) and some unknown phases are also visible for rare-earth (RE) doped alloys. The XRD pattern of has been indexed in the cubic $L2_1$ structure.

The occurrence of first-order martensitic transition in the studied alloys was examined using DSC measurements as shown in Fig. 1(b). A transition from MP/AP to AP/MP with large endothermic /exothermic peaks with thermal hysteresis was observed in the heat flow curves during heating/cooling cycles. The observed peaks arise from the latent heat of the structural transition. The values of T_M, latent heat (L) and the total entropy change (ΔS_T) associated with martensitic transition were determined and are summarized in Fig. 1(b).The martensitic transition temperature was found to increase with corresponding doping of heavy RE elements

Gd, Ho and Er relative to the undoped $Ni_{43}Mn_{46}Sn_{11}$ alloy. Interestingly, for Pr (light RE) doped alloy, a drastic shift in T_M to 270 K which is ~ 65 K shift relative to undoped compound was observed. Thus, doping small amount of RE in $Ni_{43}Mn_{46}Sn_{11}$ Heusler alloys increases the stability of martensitic phase at higher temperature.

Fig. 2 (a-e) and (f) show the M(T) curves of the alloys in applied fields of 100 Oe and 50 kOe, respectively. The FCC and FCH M(T) curves at H = 100 Oe for the parent $Ni_{43}Mn_{46}Sn_{11}$ shows that the compound is in a ferromagnetic state in both MP and AP. As the temperature increases three successive magnetic transitions are observed: (i) FM to low magnetic martensitic phase (LMMP) at T_C^M; (ii) from LMMP to a ferromagnetic austenite phase (FMAP) at the MST (T_M ~ 195 K); and (iii) from a FMAP to a paramagnetic AP at (T_C^A). A temperature hysteresis in the M(T) curves on heating (FCH) and cooling (FCC) clearly indicates a first-order structural transition (FOT) from MP to AP. The M(T) curves for the doped alloys evolve in similar manner to that of the parent alloy as shown in Fig. 2(b)-(e). However, the effect of doping can be seen in T_M. T_M shifts towards higher temperature by the corresponding substitution of Pr, Gd, Ho, and Er (see Fig 2(a)-(e) for values) with a maximum shift of ~ 60 K for $Ni_{42}PrMn_{46}Sn_{11}$ alloy at H = 100 Oe. The T_M from the magnetization measurements showed the similar variation tendency as observed from DSC measurement for all alloys. An interesting feature observed in the M(T) curves (Fig. 2 (b-e)) typical to off-stoichiometric Ni-Mn-X (X=In, Sn, Sb) Heusler alloys is splitting of ZFC and FCC curves at low temperature region below T_C^M. Such a splitting is related to magnetic inhomogeneity and results in an exchange bias (EB) effect [7, 17].

The magnetic entropy change (ΔS_M) of all alloys near the characteristic temperatures (T_M and T_C) were calculated from the isothermal M(H) curves using the Maxwell's relation, $\Delta S_M = \int_0^H \left(\frac{\partial M}{\partial T}\right)_H dH$ as shown in Fig. 3. Both direct (with negative ΔS_M values at T_C) and inverse (with

positive ΔS_M values at T_M) MCEs were observed for all alloys. A maximum entropy change of about 32, 28, 25 and 14 $Jkg^{-1}K^{-1}$ have been observed at T_M for the compounds doped with Pr, Gd, Ho and Er, respectively, with field change of 5 T. The large values of ΔS_M originate due to the sharp change in magnetization during martensitic transitions. Furthermore, since the peaks of the $\Delta S_M(T)$ curves shifts towards higher temperatures with RE doping, large inverse MCE can be obtained in a wide temperature ranges, from 195 K to 255 K which is important for application.

From the $\Delta S_M(T)$ curves, an important parameter known as refrigeration capacity (RC) has been calculated using the formula: $|(\Delta S_M)_{peak}| \times \delta T_{FWHM}$, where $\delta T_{FWHM} = T_{hot} - T_{cold}$are the temperatures that define the full-width at half-maximum of $\Delta S_M(T)$ [21]. RC is a measure of the amount of heat transferred between the hot and cold reservoirs in an ideal refrigeration cycle. Large RC values were observed with a maximum of 250 J $kg^{-1}$for Ho doped alloy at $\mu_o\Delta H = 5T$ at T_M. As shown in the inset of Fig. 3, the RC is enhanced by doping RE except for the Er doped alloy due to its lower ΔS_M value. Interestingly for Pr doped alloy (with maximum ΔS_M value), the RC value is slightly greater than parent compound (190 J kg^{-1}) because of the decrease in peak width of ΔS_M curve. The Large values of RC observed at MST illustrate the potential use of these alloys as a coolant for magnetic refrigeration.

Fig. 4(a) shows the low temperature magnetization isotherm loop of the parent $Ni_{43}Mn_{46}Sn_{11}$ and Pr, Gd doped alloys. The M(H) isotherms were obtained after the samples were cooled down to 10 K at H = 500 Oe. Shift in the hysteresis loop from origin (known as EB phenomenon) was observed in the alloys. The observed EB effect is a clear indication of the magnetic inhomogeneity in these alloys further supporting the observed splitting of M(T) curves at lower temperatures. Large EB field (H_{EB}) of 770 Oe was observed in the parent alloy. Much larger H_{EB} of 1100 Oe, 905 Oe and 942 Oe were found for the Pr, Gd and Er doped alloys. The

maximum H_{EB} obtained for the present alloy is comparable to the largest value (1170 Oe, FC = 500 Oe) reported for Ni-Mn-Sn based Heusler system [18] .

The temperature dependence of the resistivity (ρ) in 0 and 5T applied fields near T_M was studied for the alloy doped with Gd which is shown in Fig. 4(b). As can be seen on the ρ(T) curve, the alloy shows high resistivity in the MP which drops sharply at T_M to a much smaller value in the AP. The observed variation in ρ between the MP and AP of the alloy can be explained on the basis of the density of electronic states at the Fermi energy, $N(E_F)$ according tothe relationship, $\rho \sim [N(E_F)]^{-2}$ [11]. Since $N(E_F)$ in the MP is lower than in the AP, its ρ will be higher. From the ρ(T) curve, the magnetoresistance (MR) as a function of T was estimated (see inset of Fig 4(b)). The MR is defined as $MR(\%) = (\Delta\rho/\rho_o) \times 100\%$, where $\Delta\rho = [\rho(H, T) - \rho_o]$ and $\rho_o = \rho(H = 0, T)$ for a field change of 5T. Significant MR values of -20% was found for $Ni_{42}GdMn_{46}Sn_{11}$ alloy for the magnetic field change of 5 T near T_M.

CONCLUSION:

The structural, magnetic, and magnetocaloric, transport properties of $Ni_{43}Mn_{46}Sn_{11}$ and $Ni_{42}RMn_{35}Sn_{11}$ (R = Pr, Gd, Ho, and Er) alloys have been investigated. The results indicate that: (i) the alloys predominantly crystallize in the cubic $L2_1$ austenite (AP) as main phase with small trace of martensitic phase (MP); (ii) T_M shifts towards higher temperature with maximum shift of ~ 60 K by RE doping, thus stabilizing the MP at higher temperature ; (iii) large values of MCE parameters ΔS_M and RC were found that can be tuned in a wide temperature range (195 K to 255 K) (iv) large H_{EB} was found indicating magnetic inhomogeneity of the MP (v) the alloy shows significant MR values at T_M. Thus, the RE doped NiMnSn Heusler alloys can be considered as potential MCE material.

Acknowledgements: This work was supported by the U.S. Department of Energy (DOE), Office of Science, Basic Energy Sciences (BES) under Award No. DE-FG02-06ER46291 (SIU) and DE-FG02-13ER46946 (LSU).

REFERENCES:

[1] K. A. Gschneidner Jr, V. K. Pecharsky, and A. O. Tsokol Rep. Prog. Phys. **68**, 1479 (2005)

[2] A. M.Tishin and Y. I. Spichkin,The Magnetocaloric Effect and its Applications Great BritainInstitute of Physics (2003)

[3] V. K. Pecharsky and K. A. Gschneidner Jr., Phys. Rev. Lett. **78,** 4494 (1997)

[4] O. Tegus, E. Bruck, K. H. J.Buschow and F. R. de Boer, Nature **415,** 150 (2002)

[5] A.Fujita, S. Fujieda, Y. Hasegawa and K. Fukamichi, Phys. Rev. B **67,**104416 (2003)

[6] H. Wada and Y. Tanabe, Appl. Phys. Lett. **79,** 3302 (2001)

[7] I. Dubenko, M. Khan, A. K. Pathak, B. R. Gautam, S. Stadler and N. Ali, J. Magn. Magn. Mater. **321,** 754 (2009)

[8] T. Krenke, M. Acet, E. F. Wassermann, X. Moya, L. Manosa, A. planes, Phys. Rev. B 72 014412 (2005)

[9] T. Krenke, E. Duman, M. Acet, E. F. Wassermann, X. Moya, L.Mañosa, and A. Planes, Nature Mater., vol. **4**, p. 450, (2005)

[10] F. X. Hu, B. G. Sen, and J. R. Sun, Appl. Phys. Lett.76, 3460 (2000)

[11] I. Dubenko, N. Ali, S. Stadler, A. Zhukov, V. Zhukova, B. Hernando, V. Prida,V. Prudnikov, E. Ganshina, A. Granovsky, Magnetic, Novel FunctionalMagnetic Materials, Springer Series in Materials Science, 41- 82 (2016).

[12] Y. Sutou, Y. Imano, N. Koeda, T. Omori, R. Kainuma, and K. Ishida, K. Oikawa, Appl. Phys. Lett.85, 4358–4360 (2004)

[13] R. Kainuma, Y. Imano, W. Ito, Y. Sutou, H. Morito, S. Okamoto, O. Kitakami, K. Oikawa, A. Fujita, T. Kanomata, and K. Ishida, Nature **439**, 957 (2006)

[14] I. Dubenko, A. Pathak, S. Stadler, N. Ali, Ya. Kovarskii, V. N. Prudnikov, N. S. Perov, A. B. Granovsky, Phys. Rev. B **80**092408 (2009)

[15] A. K. Pathak, M. Khan, I. Dubenko, S. Stadler, and N. Ali, Appl. Phys. Lett.**90**, 262504 (2007).

[16] M. Khan, A. K. Pathak, M. R. Paudel, I. Dubenko, S. Stadler, N. Ali, J. Magn. Magn.Mater. **320,** L21-L25(2008)

[17] M. Khan, I. Dubenko, S. Stadler, N. Ali, J. App. Phys., **102**, 113914, (2007)

[18] L. Ma, W. H. Wang, J. B. Lu, J. Q. Li, C. M. Zhen, D. L. Hou, and G. H. Wu, Appl. Phys. Lett. **99**, 182507 (2011)

[19] M. Khan, I. Dubenko, S. Stadler, N. Ali, J. Phys.: Condens. Matter 16, 5259 (2004)

[20] A. Aryal, A. Quetz, S. Pandey, I. Dubenko, S. Stadler, N. Ali, J. Alloy Comp. 717, 254-259, (2017).

[21] A. Aryal, A. Quetz, C. F. Sánchez-Valdés, P. J. Ibarra-Gaytán, S. Pandey, I. Dubenko, J. L. Sánchez Llamazares, S. Stadler, N. Ali, Intermetallics, 97, 89-94 (2018).

Figure Captions:

Figure 1 (a) Room temperature X-ray diffraction (XRD) patterns of $Ni_{43}Mn_{46}Sn_{11}$ and the rare-earth doped $Ni_{42}RMn_{46}Sn_{11}$ (R = Pr, Gd, Ho, Er) alloys of nominal compositions. The XRD peaks of cubic austenite phase are indexed. The symbol "*" represents the peak from the MP. (b) DSC heat flow curves as a function of temperature. The solid arrows indicate the heating and cooling cycles.

Figure 2. The temperature dependence of the magnetization M(T) of $Ni_{43}Mn_{46}Sn_{11}$ and $Ni_{42}RMn_{46}Sn_{11}$ (R = Pr, Gd, Ho, Er) alloys on heating and cooling in an applied magnetic field of (a)-(e) 100 Oe. and (f) 50 kOe. The solid and open symbols represent the zero-field cooling (ZFC / FCH) and field-cooled-cooling (FCC) cycles, respectively.

Figure 3. Magnetic entropy changes ($-\Delta S_M$) as a function of temperature for parent and RE doped alloys near T_M and T_C^A with a magnetic field change $\mu_0\Delta H = 5T$. For clarity only $-\Delta S_M$ curves for the parent, Pr and Gd doped alloys are shown. Inset: The RC values for parent and RE doped alloys at $\mu_0\Delta H = 5T$.

Figure 4. (a) M(H) loop of $Ni_{43}Mn_{46}Sn_{11}$ and Pr, Gd doped alloys measured after the samples were cooled to 10 K at H = 500 Oe. (b) Resistivity (ρ) as a function of temperature (T) at H = 0 and 50 kOe for Gd doped alloy. Inset of (b): the magnetoresistance as a function of T.

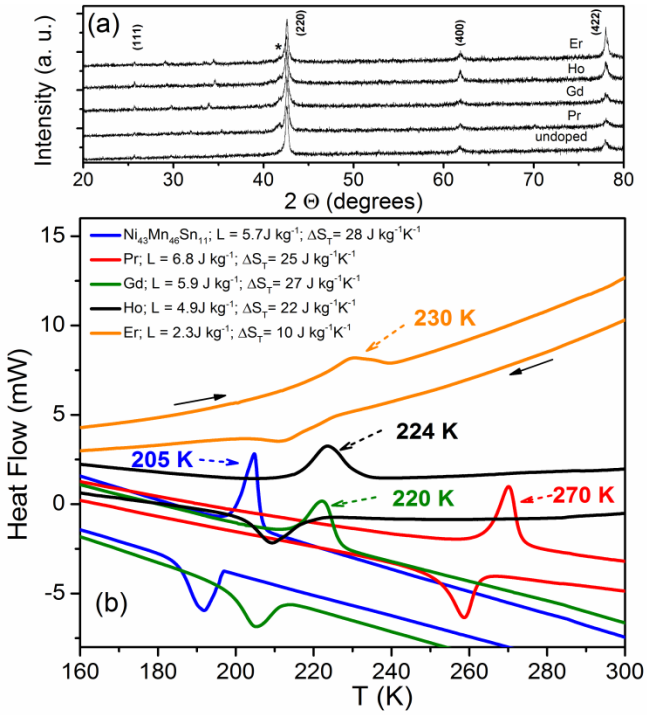

Figure 1 (a) Room temperature X-ray diffraction (XRD) patterns of $Ni_{43}Mn_{46}Sn_{11}$ and the rare-earth doped $Ni_{42}RMn_{46}Sn_{11}$ (R = Pr, Gd, Ho, Er) alloys of nominal compositions. The XRD peaks of cubic austenite phase are indexed. The symbol "*" represents the peak from the MP. (b) DSC heat flow curves as a function of temperature. The solid arrows indicate the heating and cooling cycles.

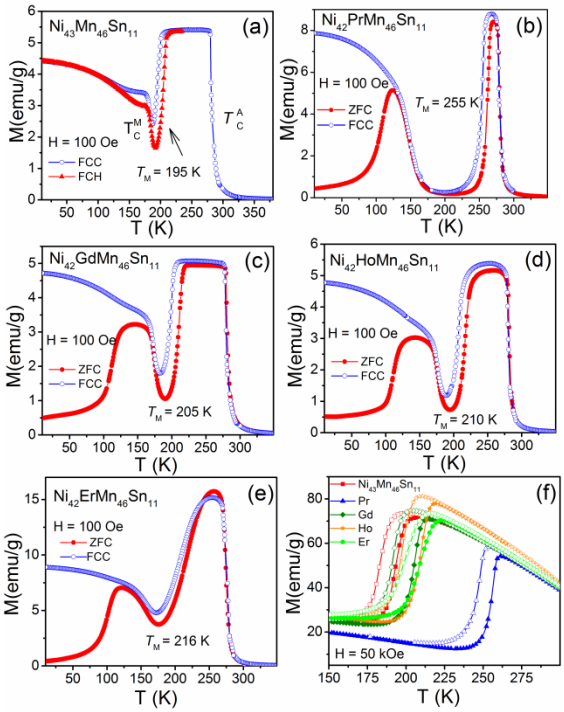

Figure 2. The temperature dependence of the magnetization M(T) of $Ni_{43}Mn_{46}Sn_{11}$ and $Ni_{42}RMn_{46}Sn_{11}$ (R = Pr, Gd, Ho, Er) alloys on heating and cooling in an applied magnetic field of (a)-(e) 100 Oe. and (f) 50 kOe. The solid and open symbols represent the zero-field cooling (ZFC / FCH) and field-cooled-cooling (FCC) cycles, respectively.

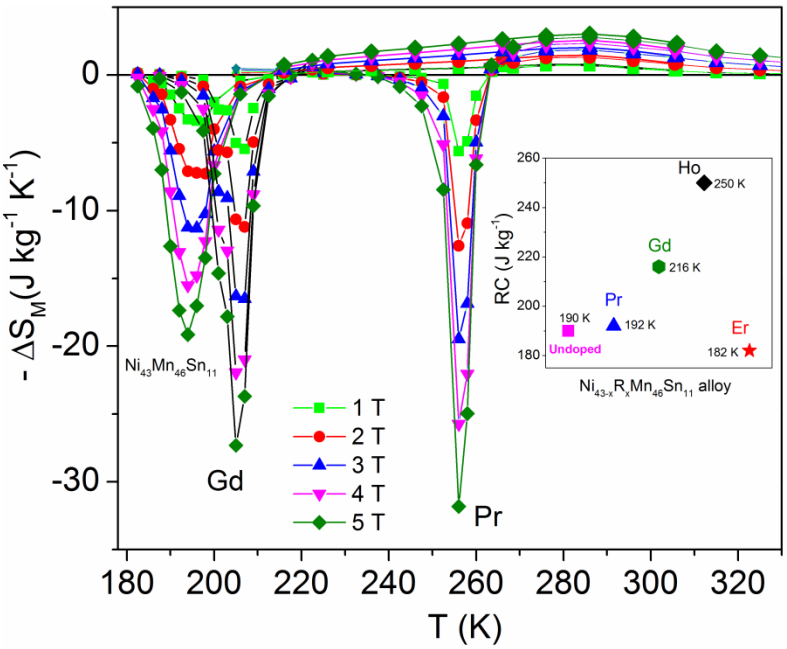

Figure 3. Magnetic entropy changes ($-\Delta S_M$) as a function of temperature for parent and RE doped alloys near T_M and T_C^A with a magnetic field change $\mu_0\Delta H = 5T$. For clarity only $-\Delta S_M$ curves for the parent, Pr and Gd doped alloys are shown. Inset: The RC values for parent and RE doped alloys at $\mu_0\Delta H = 5T$.

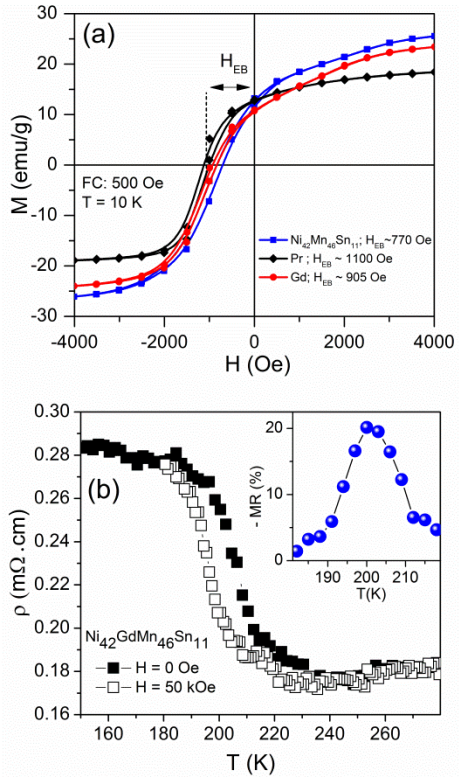

Figure 4. (a) M(H) loop of $Ni_{43}Mn_{46}Sn_{11}$ and Pr, Gd doped alloys measured after the samples were cooled to 10 K at H = 500 Oe. (b) Resistivity (ρ) as a function of temperature (T) at H = 0 and 50 kOe for Gd doped alloy. Inset of (b): the magnetoresistance as a function of T.